

AD-A273 517



(2)

OFFICE OF NAVAL RESEARCH
Grant No. N00014-91-J-1655
R&T Code 4132058---02

TECHNICAL REPORT NO. 10

Surface-Induced Static Undulations in Multilayer Films of Liquid-Crystalline Polymers

by

R.E. Geer and R. Shashidar
Center for Bio/Molecular Science and Technology
Code 6900
Naval Research Laboratory
Washington, D.C. 20375

and

A.F. Thibodeaux and R.S. Duran
Department of Chemistry
University of Florida
Gainesville, FL

S DTIC
ELECTE
DEC 07 1993
A

Reproduction in whole or in part is permitted for any purpose of the United States Government.

This document has been approved for public release and sale; its distribution is unlimited.

93-29779



93 12 6 069

REPORT DOCUMENTATION PAGE			Form Approved OMB No 0704 0188	
<small>1. This report is the property of the U.S. Government and is loaned to your agency; it and its contents are not to be distributed outside your agency. 2. This report is to be maintained in the data needed and is to be made available to the public upon request. 3. This report is to be made available to the public upon request. 4. This report is to be made available to the public upon request. 5. This report is to be made available to the public upon request. 6. This report is to be made available to the public upon request. 7. This report is to be made available to the public upon request. 8. This report is to be made available to the public upon request. 9. This report is to be made available to the public upon request. 10. This report is to be made available to the public upon request. 11. This report is to be made available to the public upon request. 12. This report is to be made available to the public upon request. 13. This report is to be made available to the public upon request. 14. This report is to be made available to the public upon request. 15. This report is to be made available to the public upon request. 16. This report is to be made available to the public upon request. 17. This report is to be made available to the public upon request. 18. This report is to be made available to the public upon request. 19. This report is to be made available to the public upon request. 20. This report is to be made available to the public upon request. 21. This report is to be made available to the public upon request. 22. This report is to be made available to the public upon request. 23. This report is to be made available to the public upon request. 24. This report is to be made available to the public upon request. 25. This report is to be made available to the public upon request. 26. This report is to be made available to the public upon request. 27. This report is to be made available to the public upon request. 28. This report is to be made available to the public upon request. 29. This report is to be made available to the public upon request. 30. This report is to be made available to the public upon request. 31. This report is to be made available to the public upon request. 32. This report is to be made available to the public upon request. 33. This report is to be made available to the public upon request. 34. This report is to be made available to the public upon request. 35. This report is to be made available to the public upon request. 36. This report is to be made available to the public upon request. 37. This report is to be made available to the public upon request. 38. This report is to be made available to the public upon request. 39. This report is to be made available to the public upon request. 40. This report is to be made available to the public upon request. 41. This report is to be made available to the public upon request. 42. This report is to be made available to the public upon request. 43. This report is to be made available to the public upon request. 44. This report is to be made available to the public upon request. 45. This report is to be made available to the public upon request. 46. This report is to be made available to the public upon request. 47. This report is to be made available to the public upon request. 48. This report is to be made available to the public upon request. 49. This report is to be made available to the public upon request. 50. This report is to be made available to the public upon request. 51. This report is to be made available to the public upon request. 52. This report is to be made available to the public upon request. 53. This report is to be made available to the public upon request. 54. This report is to be made available to the public upon request. 55. This report is to be made available to the public upon request. 56. This report is to be made available to the public upon request. 57. This report is to be made available to the public upon request. 58. This report is to be made available to the public upon request. 59. This report is to be made available to the public upon request. 60. This report is to be made available to the public upon request. 61. This report is to be made available to the public upon request. 62. This report is to be made available to the public upon request. 63. This report is to be made available to the public upon request. 64. This report is to be made available to the public upon request. 65. This report is to be made available to the public upon request. 66. This report is to be made available to the public upon request. 67. This report is to be made available to the public upon request. 68. This report is to be made available to the public upon request. 69. This report is to be made available to the public upon request. 70. This report is to be made available to the public upon request. 71. This report is to be made available to the public upon request. 72. This report is to be made available to the public upon request. 73. This report is to be made available to the public upon request. 74. This report is to be made available to the public upon request. 75. This report is to be made available to the public upon request. 76. This report is to be made available to the public upon request. 77. This report is to be made available to the public upon request. 78. This report is to be made available to the public upon request. 79. This report is to be made available to the public upon request. 80. This report is to be made available to the public upon request. 81. This report is to be made available to the public upon request. 82. This report is to be made available to the public upon request. 83. This report is to be made available to the public upon request. 84. This report is to be made available to the public upon request. 85. This report is to be made available to the public upon request. 86. This report is to be made available to the public upon request. 87. This report is to be made available to the public upon request. 88. This report is to be made available to the public upon request. 89. This report is to be made available to the public upon request. 90. This report is to be made available to the public upon request. 91. This report is to be made available to the public upon request. 92. This report is to be made available to the public upon request. 93. This report is to be made available to the public upon request. 94. This report is to be made available to the public upon request. 95. This report is to be made available to the public upon request. 96. This report is to be made available to the public upon request. 97. This report is to be made available to the public upon request. 98. This report is to be made available to the public upon request. 99. This report is to be made available to the public upon request. 100. This report is to be made available to the public upon request. 101. This report is to be made available to the public upon request. 102. This report is to be made available to the public upon request. 103. This report is to be made available to the public upon request. 104. This report is to be made available to the public upon request. 105. This report is to be made available to the public upon request. 106. This report is to be made available to the public upon request. 107. This report is to be made available to the public upon request. 108. This report is to be made available to the public upon request. 109. This report is to be made available to the public upon request. 110. This report is to be made available to the public upon request. 111. This report is to be made available to the public upon request. 112. This report is to be made available to the public upon request. 113. This report is to be made available to the public upon request. 114. This report is to be made available to the public upon request. 115. This report is to be made available to the public upon request. 116. This report is to be made available to the public upon request. 117. This report is to be made available to the public upon request. 118. This report is to be made available to the public upon request. 119. This report is to be made available to the public upon request. 120. This report is to be made available to the public upon request. 121. This report is to be made available to the public upon request. 122. This report is to be made available to the public upon request. 123. This report is to be made available to the public upon request. 124. This report is to be made available to the public upon request. 125. This report is to be made available to the public upon request. 126. This report is to be made available to the public upon request. 127. This report is to be made available to the public upon request. 128. This report is to be made available to the public upon request. 129. This report is to be made available to the public upon request. 130. This report is to be made available to the public upon request. 131. This report is to be made available to the public upon request. 132. This report is to be made available to the public upon request. 133. This report is to be made available to the public upon request. 134. This report is to be made available to the public upon request. 135. This report is to be made available to the public upon request. 136. This report is to be made available to the public upon request. 137. This report is to be made available to the public upon request. 138. This report is to be made available to the public upon request. 139. This report is to be made available to the public upon request. 140. This report is to be made available to the public upon request. 141. This report is to be made available to the public upon request. 142. This report is to be made available to the public upon request. 143. This report is to be made available to the public upon request. 144. This report is to be made available to the public upon request. 145. This report is to be made available to the public upon request. 146. This report is to be made available to the public upon request. 147. This report is to be made available to the public upon request. 148. This report is to be made available to the public upon request. 149. This report is to be made available to the public upon request. 150. This report is to be made available to the public upon request. 151. This report is to be made available to the public upon request. 152. This report is to be made available to the public upon request. 153. This report is to be made available to the public upon request. 154. This report is to be made available to the public upon request. 155. This report is to be made available to the public upon request. 156. This report is to be made available to the public upon request. 157. This report is to be made available to the public upon request. 158. This report is to be made available to the public upon request. 159. This report is to be made available to the public upon request. 160. This report is to be made available to the public upon request. 161. This report is to be made available to the public upon request. 162. This report is to be made available to the public upon request. 163. This report is to be made available to the public upon request. 164. This report is to be made available to the public upon request. 165. This report is to be made available to the public upon request. 166. This report is to be made available to the public upon request. 167. This report is to be made available to the public upon request. 168. This report is to be made available to the public upon request. 169. This report is to be made available to the public upon request. 170. This report is to be made available to the public upon request. 171. This report is to be made available to the public upon request. 172. This report is to be made available to the public upon request. 173. This report is to be made available to the public upon request. 174. This report is to be made available to the public upon request. 175. This report is to be made available to the public upon request. 176. This report is to be made available to the public upon request. 177. This report is to be made available to the public upon request. 178. This report is to be made available to the public upon request. 179. This report is to be made available to the public upon request. 180. This report is to be made available to the public upon request. 181. This report is to be made available to the public upon request. 182. This report is to be made available to the public upon request. 183. This report is to be made available to the public upon request. 184. This report is to be made available to the public upon request. 185. This report is to be made available to the public upon request. 186. This report is to be made available to the public upon request. 187. This report is to be made available to the public upon request. 188. This report is to be made available to the public upon request. 189. This report is to be made available to the public upon request. 190. This report is to be made available to the public upon request. 191. This report is to be made available to the public upon request. 192. This report is to be made available to the public upon request. 193. This report is to be made available to the public upon request. 194. This report is to be made available to the public upon request. 195. This report is to be made available to the public upon request. 196. This report is to be made available to the public upon request. 197. This report is to be made available to the public upon request. 198. This report is to be made available to the public upon request. 199. This report is to be made available to the public upon request. 200. This report is to be made available to the public upon request.</small>				
1. AGENCY USE ONLY (Leave blank)		2. REPORT DATE 10/20/93	3. REPORT TYPE AND DATES COVERED Technical	
4. TITLE AND SUBTITLE Surface-Induced Static Undulations in Multilayer Films of Liquid-Crystalline Polymers			5. FUNDING NUMBERS N00014-91-J-1655	
6. AUTHOR(S) R.E. Geer, R. Shashidar, A.F. Thibodeaux and R.S. Duran				
7. PERFORMING ORGANIZATION NAME(S) AND ADDRESS(ES) R. S. Duran Department of Chemistry University of Florida Gainesville, FL 32611-7200			8. PERFORMING ORGANIZATION REPORT NUMBER 10	
9. SPONSORING / MONITORING AGENCY NAME(S) AND ADDRESS(ES) Dr. Kenneth J. Wynne Code 1113PO, Office of the Chief of Naval Research 800 North Quincy Street Arlington, VA 22217-5000 (703) 696-4409			10. SPONSORING / MONITORING AGENCY REPORT NUMBER	
11. SUPPLEMENTARY NOTES submitted to Phys. Rev. Lett.				
12a. DISTRIBUTION / AVAILABILITY STATEMENT			12b. DISTRIBUTION CODE	
13. ABSTRACT (Maximum 200 words) The first detailed study of surface-induced undulations in a liquid-crystalline polymer is presented. By examining the non-specular diffuse scattering from a 30-layer film of ferroelectric liquid-crystal polymer it is shown that the layer fluctuations are induced by the roughness of the film/substrate interface. This is in contrast to the case of free-standing films wherein thermal fluctuations play the major role.				
14. SUBJECT TERMS			15. NUMBER OF PAGES	
			16. PRICE CODE	
17. SECURITY CLASSIFICATION OF REPORT Unclassified		18. SECURITY CLASSIFICATION OF THIS PAGE Unclassified	19. SECURITY CLASSIFICATION OF ABSTRACT Unclassified	
20. LIMITATION OF ABSTRACT				

SUBMITTED PHYS. REV. LETT.
**Surface-Induced Static Undulations in Multilayer Films of Liquid-
Crystalline Polymers**

R. E. Geer and R. Shashidhar
Center for Bio/Molecular Science and Technology, Code 6900,
Naval Research Laboratory, Washington, D.C. 20375

A. F. Thibodeaux and R. S. Duran
Department of Chemistry, University of Florida, Gainesville, Fl

Abstract

The first detailed study of surface-induced undulations in a liquid-crystalline polymer is presented. By examining the non-specular diffuse scattering from a 30-layer film of ferroelectric liquid-crystal polymer it is shown that the layer fluctuations are induced by the roughness of the film/substrate interface. This is in contrast to the case of free-standing films wherein thermal fluctuations play the major role.

Thin, smectic liquid-crystal films are of considerable current interest since they serve as model systems to study two-dimensional to three-dimensional crossover of inter- and intralayer order. For the most part, these studies have been on free-standing films. It is equally important to understand the influence of the interface between liquid-crystal films and the substrate. Film/vacuum and film/substrate interfaces are known to induce structural changes which are localized in the interfacial regions. On the other hand, such interfaces can also induce distinct thermodynamic phases as well as static undulations which penetrate into the interior of the film. The static undulations induced by roughness of the substrate surface has been studied in thin adsorbed films of cyclohexane. It was shown that for very thin films the substrate van der Waals interactions constrain the liquid surface to follow the static undulations of the substrate surface, while for thicker films the liquid surface structure is influenced mainly by thermally induced capillary waves. Early studies in homeotropically aligned smectic-

DTIC QUALITY INSPECTED 3

Dist

A-1

odes

for

Special

imperfections associated with the smectic layer order. Rocking scans through this diffuse scattering are shown in Fig. 2 for the first three Bragg peaks of Fig. 1. *These scans consist of broad diffuse scattering accompanied by a resolution limited peak due to specular reflection.* It may be recalled that Davidson and Levelut have reported similar diffuse bands perpendicular to the OOL axis for bulk samples of polysiloxane liquid-crystal polymers. These bands were attributed to undulations of longitudinally correlated rows of mesogens. The widths and amplitudes of the diffuse peaks of our LB multilayer shown in Fig. 1 are not consistent with such longitudinal undulations. We shall show that the diffuse scattering for the liquid-crystalline polymer is in fact due to static undulations of the smectic layers induced by the roughness of the substrate surface.

Quantitative analysis of the diffuse scattering of Fig. 2 is similar to that used by Sinha et al. for solid surfaces.⁷ For a single rough surface, the scattered intensity is given by

$$S(\vec{q}) = \frac{1}{q_z^2} \iint_{S_0} dX dY e^{q_z^2 C(X,Y)} e^{-i(q_x X + q_y Y)} .$$

X and Y are the Cartesian separations of two points on the surface S_0 with an average layer normal in the \hat{z} direction. $C(X,Y)$ is the surface height-height correlation function. This is related to the average roughness across the sample $g(X,Y) = \langle [z(X,Y) - z(0)]^2 \rangle$. For many isotropic solid surfaces $g(R = (X^2 + Y^2)^{1/2}) = AR^{2h}$ describing so-called self-affine roughness¹⁸. $h = D_H - 3$, where D_H is the fractal dimension of the surface. For systems of finite size (and measurement techniques with limited spatial resolution) $g(R) \rightarrow 2\sigma^2$ for large R , where σ is the rms roughness of the surface. A functional form satisfying these limits is

$$g(R) = 2\sigma^2 [1 - e^{-(R/\xi)^{2h}}] .$$

ξ is a long-distance cutoff. Using this form for $g(R)$,

$$C(R) = \sigma^2 e^{-(R/\xi)^{2h}} .$$

$F(q_z)$ was determined by the specular portion of the rocking curves, the rms interlayer roughness σ , and the resolution function of the spectrometer. The fits are shown as solid lines in Fig. 2. *The agreement is excellent for all three rocking curves.* The data for all three quasi-Bragg peaks in Fig. 2 were fit using only *three significant adjustable parameters*: σ , ξ and h . Their values obtained from best fits are 3.6 ± 0.12 Å, 1327 ± 18 Å and 0.25 ± 0.05 , respectively. It should be mentioned that the wide range of q_z and q_x for the rocking curve data makes the fits extremely sensitive to the value of h . Figure 3, which plots the central portion of the 002 rocking curve with fits for three different values of h , demonstrates this sensitivity.

Thermally induced layer undulations also contribute to the diffuse scattering from the multilayer. To estimate this contribution, the layer displacement correlation function was calculated following Holyst⁶. Using the above values of B and K used to estimate L , and air/film and film/substrate interfacial tensions of 30 dyn/cm and 10 dyn/cm, respectively, the layer displacement correlation function, $\langle u_{lh}(R)u_{lh}(0) \rangle$ for the center of a 30-layer film is plotted in Fig. 5. Such thermal induced fluctuations are not conformal i.e. $C_{ij}(R)$ decays quickly for $i \neq j$ ⁶. Hence this estimate represents an upper limit. For comparison, the layer undulation correlation function determined by the fits to the data in Fig. 2 is also plotted.

Consider, instead the penetration of static undulations through the film. As stated above, the large value of the compression modulus in these liquid-crystal polymer films induces a large smectic penetration depth L . It is energetically less costly to propagate layer undulations parallel to the layer normal at the expense of in-plane director splay. Hence substrate roughness plays a major role in the smectic layer structure. The specular reflectivity of x-rays from the silicon substrate was measured to characterize its surface roughness. The substrate consists of a monolayer of octadecyltrichlorosilane (OTS) chemisorbed to the native oxide of a polished (100) silicon wafer. This data is shown in Fig. 4, along with the corresponding electron density profile. The data and fit agree very well with previous results on OTS coated silicon obtained by Tidswell et al.³ The modeling technique has been thoroughly discussed in Ref. [3]. The analysis yields an alkyl chain region with a density $\rho/\rho_{Si} = 0.38 \pm 0.03$ and a thickness of 21 ± 0.5 Å, indicative of a well-formed monolayer with a maximum chain tilt of 22° . As is the case with homeotropic alignment of bulk liquid-crystal samples by alkylsilanes,

Figure captions:

Figure 1. Specular and off-specular scans for a 29-layer liquid-crystal polymer film. The latter has been offset by a factor of five for clarity. Four Bragg reflections (layer spacing $c=45.7$ Å) are evident in the specular data revealing a well ordered layer structure. The mosaic of the layer normal is limited to 0.07° . The q_z dependence of the amplitude of the subsidiary maxima is discussed in Ref. [1]. The off-specular scan was taken at a trajectory $q_x=0.006q_z$. Diffuse scattering, sharply peaked at q_z of the Bragg reflections, is evident. The width of these peaks are similar to the primary maxima of the specular scan, implying that the associated layer undulations are replicated layer to layer. Inset shows chemical structure of the copolymer.

Figure 2. Rocking scans across the (a) 001, (b) 002 and (c) 003 Bragg reflections of Fig. 1. The incident beam in (a) was attenuated to avoid detector saturation near the peak. Open circles denote experimental data. Solid lines represent best fits to the model described in the text.

Figure 3. Enlargement of data and best fits to the 002 rocking curve for different values of h . Solid line: $h=0.25$, short dashed line: $h=1$, dashed-dot-dot line: $h=2$. All fits have been convolved with instrumental resolution. Inset: interfacial undulation correlation functions determined from fits to the rocking curve data (circles) and calculated from the model of Holyst for thermal undulations (triangles). The latter, calculated at the midpoint of a 29-layer film with $K=1 \times 10^{-6}$ dyn, $B=2.5 \times 10^9$ dyn/cm², $\gamma_{air/film}=30$ dyn/cm and $\gamma_{film/substrate}=10$ dyn/cm. The compressibility of the interdigitated layer consisting of the side-chain mesogens and alkyl chains of the silanes, $B_0=2.5 \times 10^7$ dyn/cm².

Figure 4. Specular reflectivity normalized to Fresnel reflectivity (open circles) and fit to the model of Ref. [3] (solid line). The corresponding electron density profile is shown in the inset.

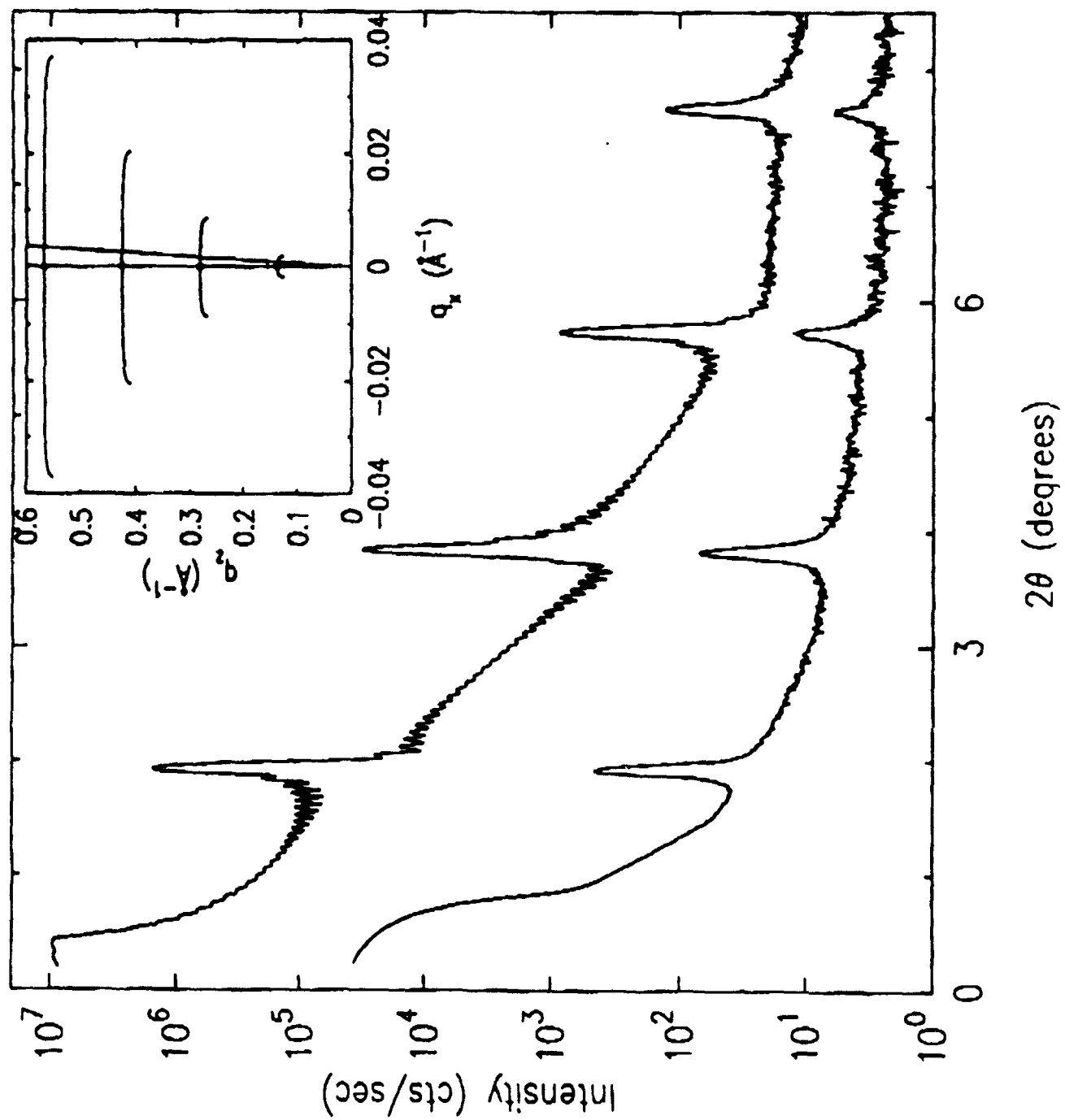
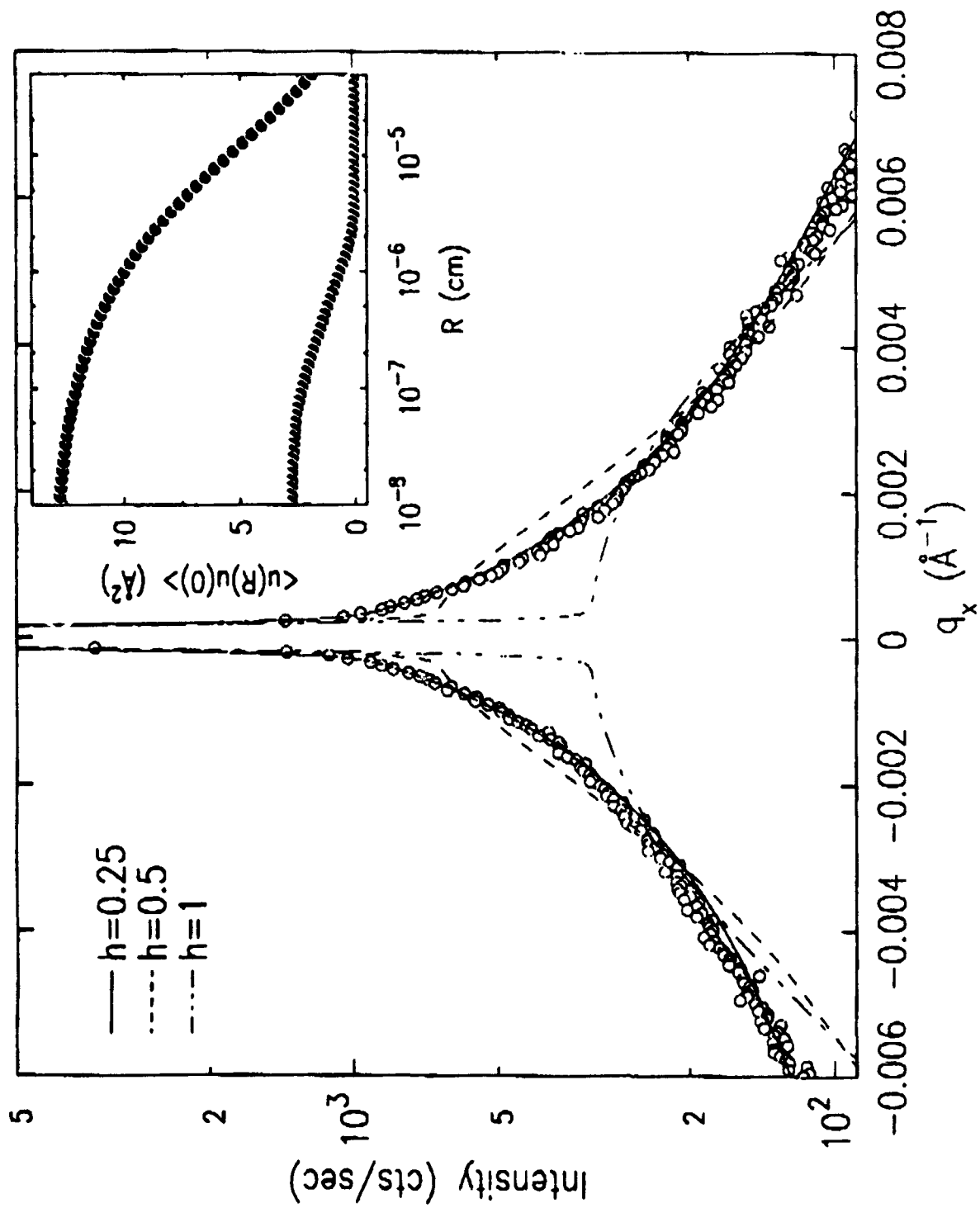


Fig. 1



Surface-Induced Static Undulations in Multilayer Films of Liquid-Crystalline Polymers

R. E. Geer and R. Shashidhar

Center for Bio/Molecular Science and Technology, Code 6900,
Naval Research Laboratory, Washington, D.C. 20375

A. F. Thibodeaux and R. S. Duran

Department of Chemistry, University of Florida, Gainesville, FL

Abstract

The first detailed study of surface-induced undulations in a liquid-crystalline polymer is presented. By examining the non-specular diffuse scattering from a 30-layer film of ferroelectric liquid-crystal polymer it is shown that the layer fluctuations are induced by the roughness of the film/substrate interface. This is in contrast to the case of free-standing films wherein thermal fluctuations play the major role.

Thin, smectic liquid-crystal films are of considerable current interest since they serve as model systems to study two-dimensional to three-dimensional crossover of inter- and intralayer order. For the most part, these studies have been on free-standing films. It is equally important to understand the influence of the interface between liquid-crystal films and the substrate. Film/vacuum and film/substrate interfaces are known to induce structural changes which are localized in the interfacial regions. On the other hand, such interfaces can also induce distinct thermodynamic phases as well as static undulations which penetrate into the interior of the film. The static undulations induced by roughness of the substrate surface has been studied in thin adsorbed films of cyclohexane. It was shown that for very thin films the substrate van der Waals interactions constrain the liquid surface to follow the static undulations of the substrate surface, while for thicker films the liquid surface structure is influenced mainly by thermally induced capillary waves. Early studies in homeotropically aligned smectic-

imperfections associated with the smectic layer order. Rocking scans through this diffuse scattering are shown in Fig. 2 for the first three Bragg peaks of Fig. 1. *These scans consist of broad diffuse scattering accompanied by a resolution limited peak due to specular reflection.* It may be recalled that Davidson and Levelut have reported similar diffuse bands perpendicular to the OOL axis for bulk samples of polysiloxane liquid-crystal polymers. These bands were attributed to undulations of longitudinally correlated rows of mesogens. The widths and amplitudes of the diffuse peaks of our LB multilayer shown in Fig. 1 are not consistent with such longitudinal undulations. We shall show that the diffuse scattering for the liquid-crystalline polymer is in fact due to static undulations of the smectic layers induced by the roughness of the substrate surface.

Quantitative analysis of the diffuse scattering of Fig. 2 is similar to that used by Sinha et al. for solid surfaces.⁷ For a single rough surface, the scattered intensity is given by

$$S(\bar{q}) = \frac{1}{q_z^2} \iint_{S_0} dX dY e^{q_z^2 C(X,Y)} e^{-i(q_x X + q_y Y)}.$$

X and Y are the Cartesian separations of two points on the surface S_0 with an average layer normal in the \hat{z} direction. $C(X,Y)$ is the surface height-height correlation function. This is related to the average roughness across the sample $g(X,Y) = \langle [z(X,Y) - z(0)]^2 \rangle$. For many isotropic solid surfaces $g(R = (X^2 + Y^2)^{1/2}) = AR^{2h}$ describing so-called self-affine roughness¹⁸. $h = D_H - 3$, where D_H is the fractal dimension of the surface. For systems of finite size (and measurement techniques with limited spatial resolution) $g(R) \rightarrow 2\sigma^2$ for large R , where σ is the rms roughness of the surface. A functional form satisfying these limits is

$$g(R) = 2\sigma^2 [1 - e^{-(R/\xi)^{2h}}].$$

ξ is a long-distance cutoff. Using this form for $g(R)$,

$$C(R) = \sigma^2 e^{-(R/\xi)^{2h}}.$$

$F(q_z)$ was determined by the specular portion of the rocking curves, the rms interlayer roughness σ , and the resolution function of the spectrometer. The fits are shown as solid lines in Fig. 2. *The agreement is excellent for all three rocking curves.* The data for all three quasi-Bragg peaks in Fig. 2 were fit using only *three significant adjustable parameters*: σ , ξ and h . Their values obtained from best fits are 3.6 ± 0.12 Å, 1327 ± 18 Å and 0.25 ± 0.05 , respectively. It should be mentioned that the wide range of q_z and q_x for the rocking curve data makes the fits extremely sensitive to the value of h . Figure 3, which plots the central portion of the 002 rocking curve with fits for three different values of h , demonstrates this sensitivity.

Thermally induced layer undulations also contribute to the diffuse scattering from the multilayer. To estimate this contribution, the layer displacement correlation function was calculated following Holyst⁶. Using the above values of B and K used to estimate L , and air/film and film/substrate interfacial tensions of 30 dyn/cm and 10 dyn/cm, respectively, the layer displacement correlation function, $\langle u_{ih}(R)u_{ih}(0) \rangle$ for the center of a 30-layer film is plotted in Fig. 5. Such thermal induced fluctuations are not conformal i.e. $C_{ij}(R)$ decays quickly for $i \neq j$ ⁶. Hence this estimate represents an upper limit. For comparison, the layer undulation correlation function determined by the fits to the data in Fig. 2 is also plotted.

Consider, instead the penetration of static undulations through the film. As stated above, the large value of the compression modulus in these liquid-crystal polymer films induces a large smectic penetration depth L . It is energetically less costly to propagate layer undulations parallel to the layer normal at the expense of in-plane director splay. Hence substrate roughness plays a major role in the smectic layer structure. The specular reflectivity of x-rays from the silicon substrate was measured to characterize its surface roughness. The substrate consists of a monolayer of octadecyltrichlorosilane (OTS) chemisorbed to the native oxide of a polished (100) silicon wafer. This data is shown in Fig. 4, along with the corresponding electron density profile. The data and fit agree very well with previous results on OTS coated silicon obtained by Tidswell et al.³ The modeling technique has been thoroughly discussed in Ref. [3]. The analysis yields an alkyl chain region with a density $\rho/\rho_{Si} = 0.38 \pm 0.03$ and a thickness of 21 ± 0.5 Å, indicative of a well-formed monolayer with a maximum chain tilt of 22°. As is the case with homeotropic alignment of bulk liquid-crystal samples by alkylsilanes,

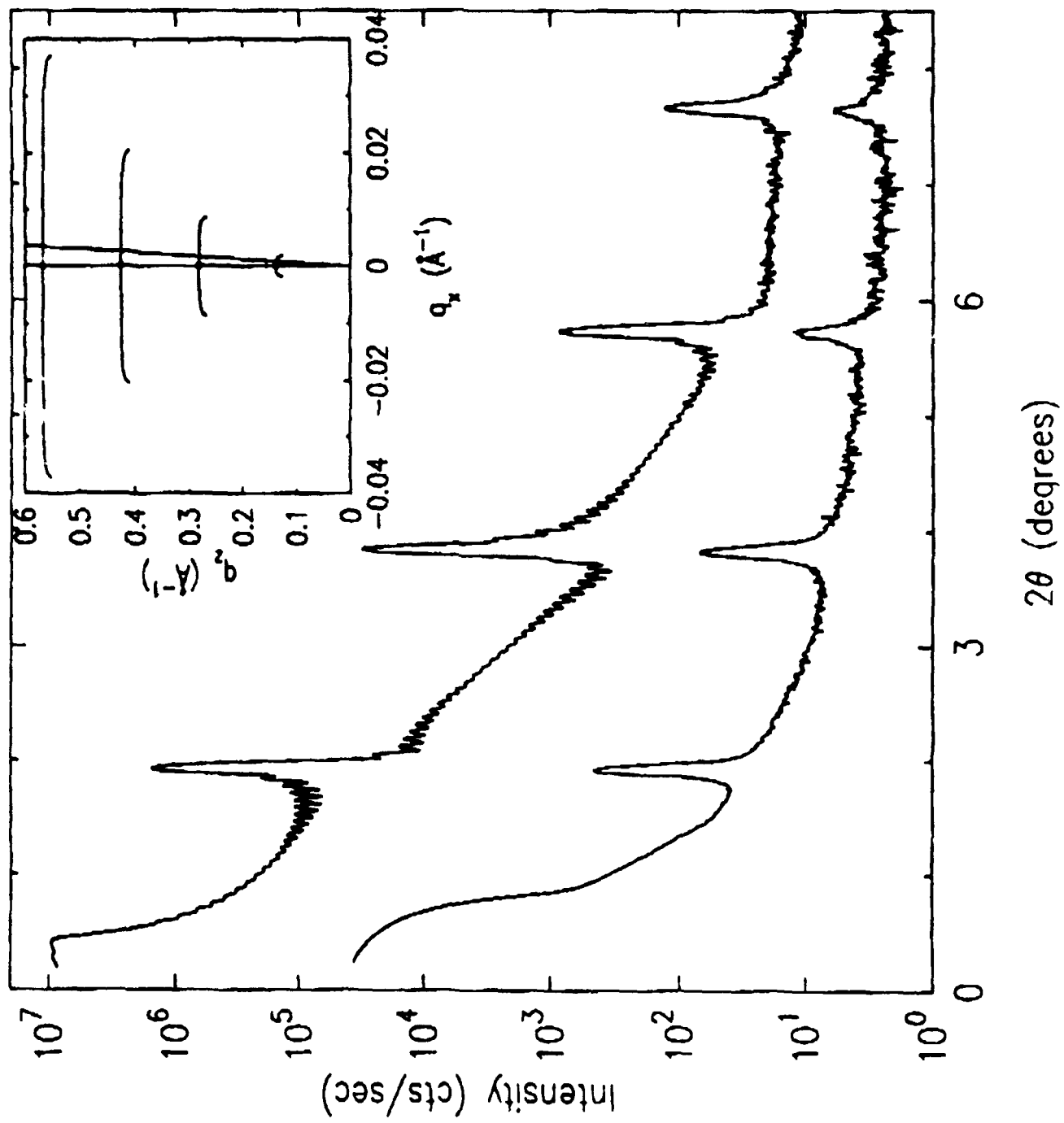
Figure captions:

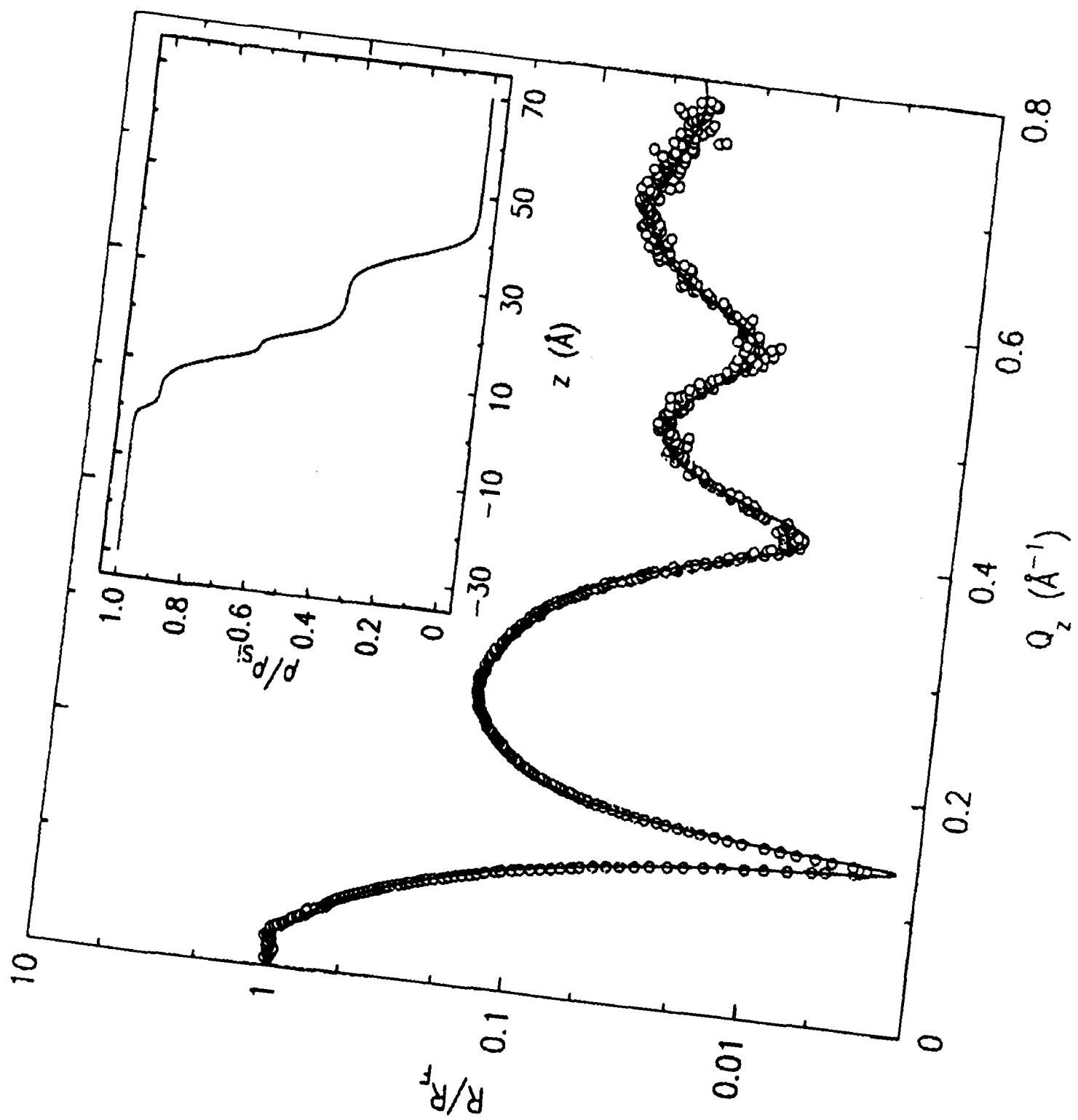
Figure 1. Specular and off-specular scans for a 29-layer liquid-crystal polymer film. The latter has been offset by a factor of five for clarity. Four Bragg reflections (layer spacing $c=45.7 \text{ \AA}$) are evident in the specular data revealing a well ordered layer structure. The mosaic of the layer normal is limited to 0.07° . The q_z dependence of the amplitude of the subsidiary maxima is discussed in Ref. [1]. The off-specular scan was taken at a trajectory $q_x=0.006q_z$. Diffuse scattering, sharply peaked at q_z of the Bragg reflections, is evident. The width of these peaks are similar to the primary maxima of the specular scan, implying that the associated layer undulations are replicated layer to layer. Inset shows chemical structure of the copolymer.

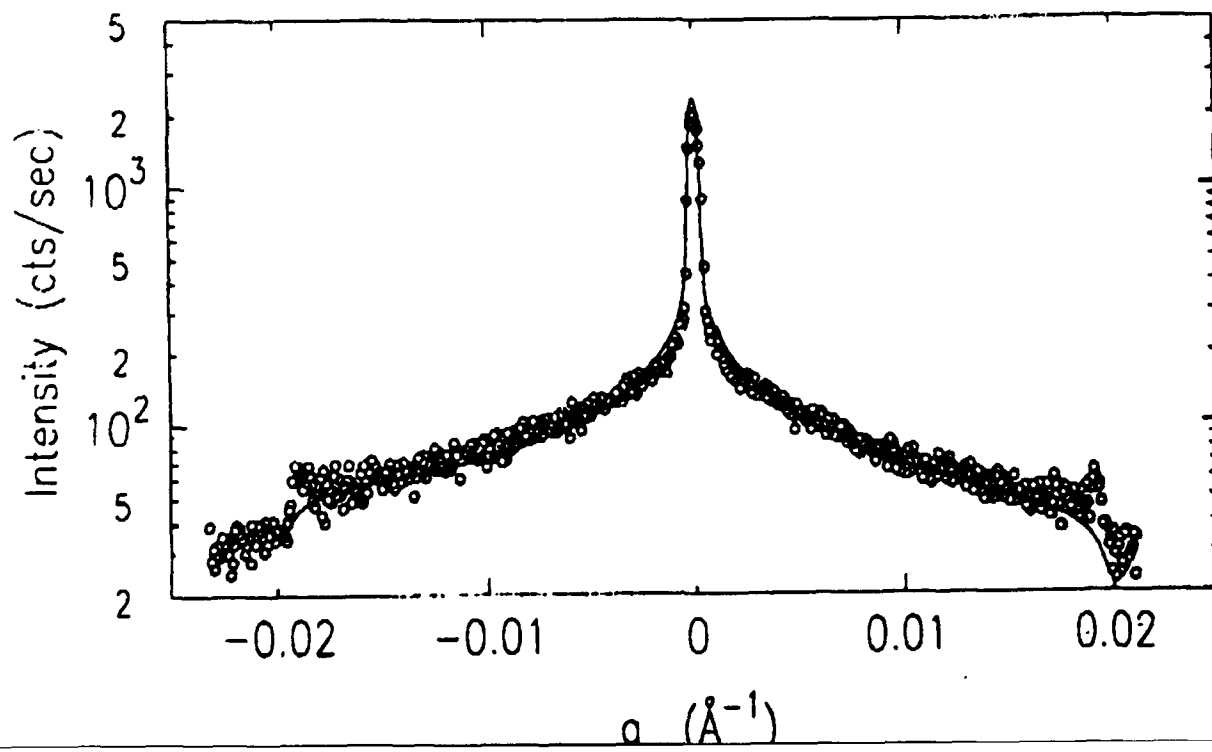
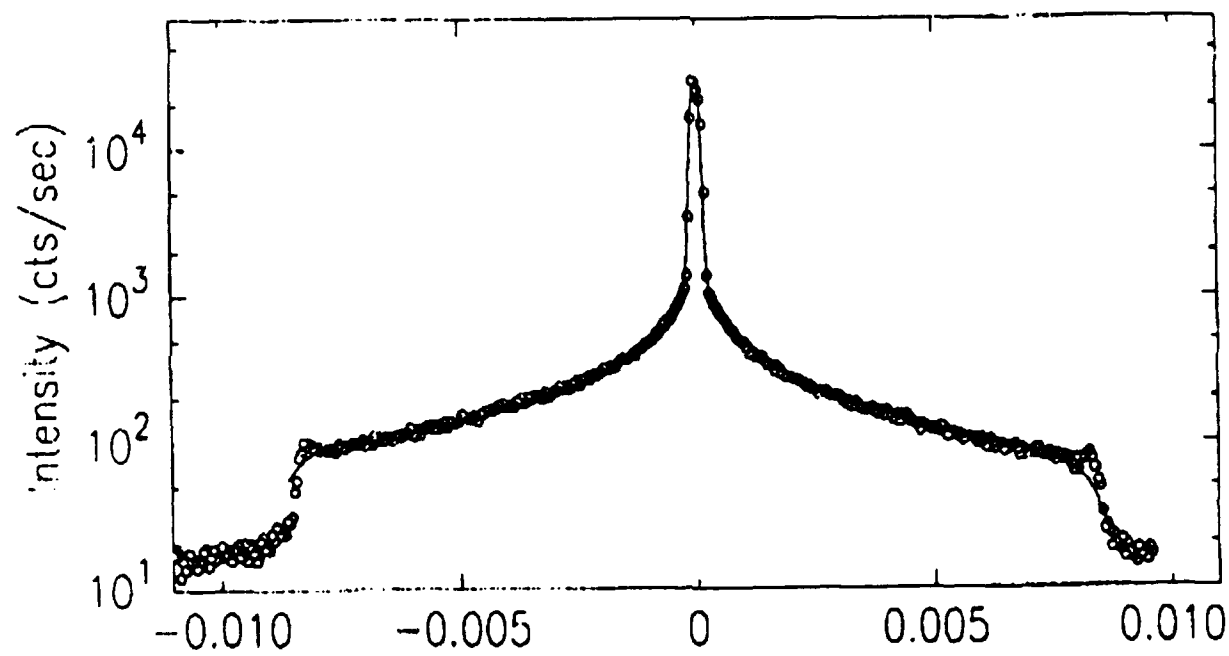
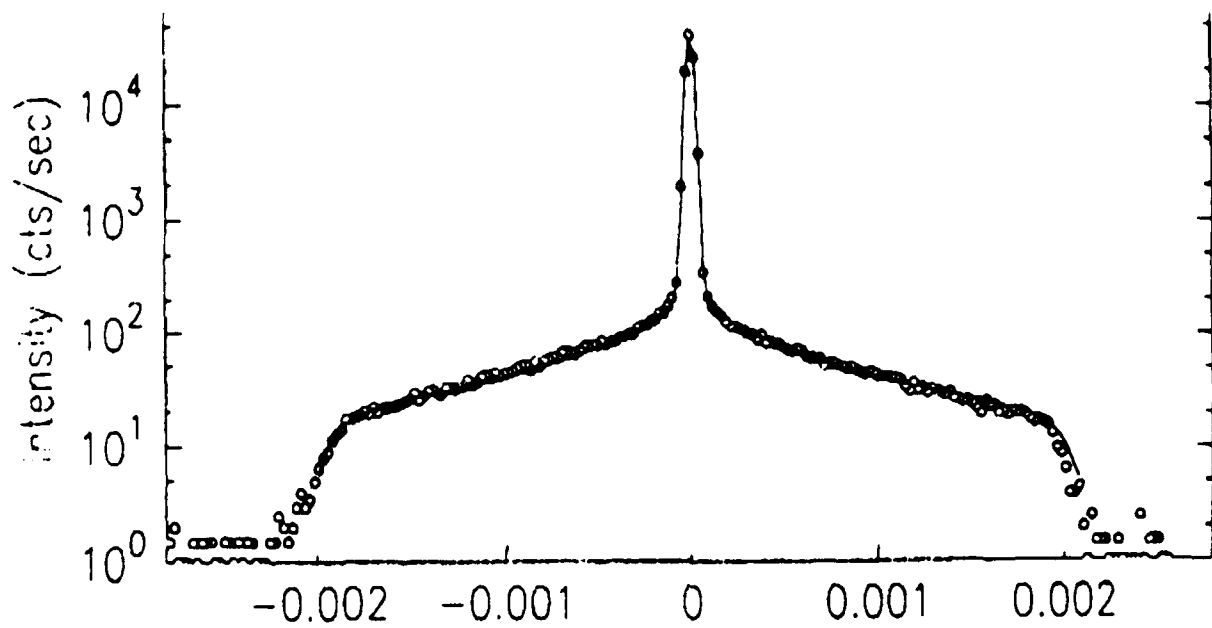
Figure 2. Rocking scans across the (a) 001, (b) 002 and (c) 003 Bragg reflections of Fig. 1. The incident beam in (a) was attenuated to avoid detector saturation near the peak. Open circles denote experimental data. Solid lines represent best fits to the model described in the text.

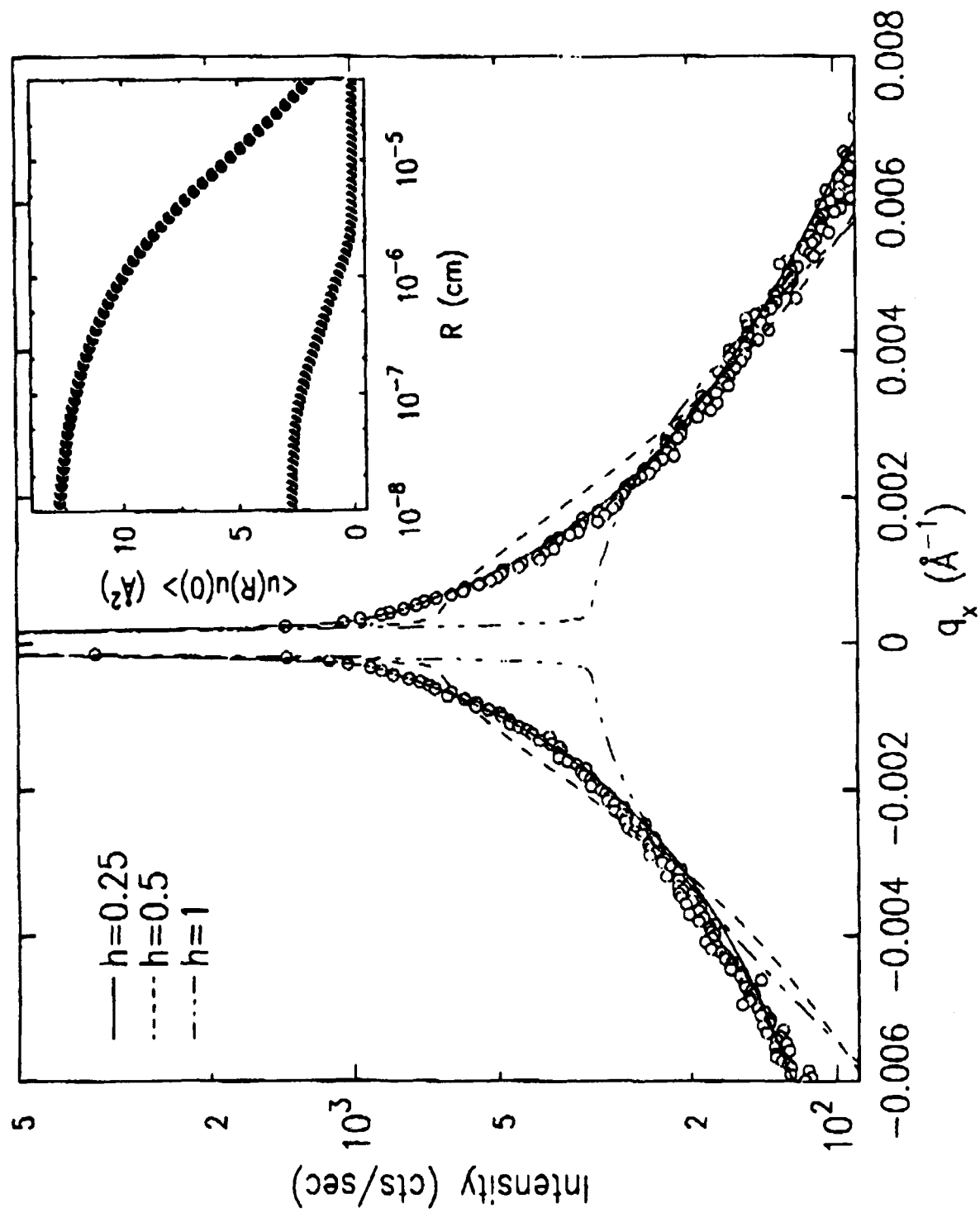
Figure 3. Enlargement of data and best fits to the 002 rocking curve for different values of h . Solid line: $h=0.25$, short dashed line: $h=1$, dashed-dot-dot line: $h=2$. All fits have been convolved with instrumental resolution. Inset: interfacial undulation correlation functions determined from fits to the rocking curve data (circles) and calculated from the model of Holyst for thermal undulations (triangles). The latter, calculated at the midpoint of a 29-layer film with $K=1 \times 10^{-6} \text{ dyn}$, $B=2.5 \times 10^9 \text{ dyn/cm}^2$, $\gamma_{\text{air/film}}=30 \text{ dyn/cm}$ and $\gamma_{\text{film/substrate}}=10 \text{ dyn/cm}$. The compressibility of the interdigitated layer consisting of the side-chain mesogens and alkyl chains of the silanes, $B_o=2.5 \times 10^7 \text{ dyn/cm}^2$.

Figure 4. Specular reflectivity normalized to Fresnel reflectivity (open circles) and fit to the model of Ref. [3] (solid line). The corresponding electron density profile is shown in the inset.









SUBMITTED PHYS. REV. LETT.
**Surface-Induced Static Undulations in Multilayer Films of Liquid-
Crystalline Polymers**

R. E. Geer and R. Shashidhar
Center for Bio/Molecular Science and Technology, Code 6900,
Naval Research Laboratory, Washington, D.C. 20375

A. F. Thibodeaux and R. S. Duran
Department of Chemistry, University of Florida, Gainesville, Fl

Abstract

The first detailed study of surface-induced undulations in a liquid-crystalline polymer is presented. By examining the non-specular diffuse scattering from a 30-layer film of ferroelectric liquid-crystal polymer it is shown that the layer fluctuations are induced by the roughness of the film/substrate interface. This is in contrast to the case of free-standing films wherein thermal fluctuations play the major role.

Thin, smectic liquid-crystal films are of considerable current interest since they serve as model systems to study two-dimensional to three-dimensional crossover of inter- and intralayer order. For the most part, these studies have been on free-standing films. It is equally important to understand the influence of the interface between liquid-crystal films and the substrate. Film/vacuum and film/substrate interfaces are known to induce structural changes which are localized in the interfacial regions. On the other hand, such interfaces can also induce distinct thermodynamic phases as well as static undulations which penetrate into the interior of the film. The static undulations induced by roughness of the substrate surface has been studied in thin adsorbed films of cyclohexane. It was shown that for very thin films the substrate van der Waals interactions constrain the liquid surface to follow the static undulations of the substrate surface, while for thicker films the liquid surface structure is influenced mainly by thermally induced capillary waves. Early studies in homeotropically aligned smectic-

imperfections associated with the smectic layer order. Rocking scans through this diffuse scattering are shown in Fig. 2 for the first three Bragg peaks of Fig. 1. *These scans consist of broad diffuse scattering accompanied by a resolution limited peak due to specular reflection.* It may be recalled that Davidson and Levelut have reported similar diffuse bands perpendicular to the OOL axis for bulk samples of polysiloxane liquid-crystal polymers. These bands were attributed to undulations of longitudinally correlated rows of mesogens. The widths and amplitudes of the diffuse peaks of our LB multilayer shown in Fig. 1 are not consistent with such longitudinal undulations. We shall show that the diffuse scattering for the liquid-crystalline polymer is in fact due to static undulations of the smectic layers induced by the roughness of the substrate surface.

Quantitative analysis of the diffuse scattering of Fig. 2 is similar to that used by Sinha et al. for solid surfaces.⁷ For a single rough surface, the scattered intensity is given by

$$S(\vec{q}) = \frac{1}{q_z^2} \iint_{S_0} dX dY e^{q_z^2 C(X,Y)} e^{-i(q_x X + q_y Y)}.$$

X and Y are the Cartesian separations of two points on the surface S_0 with an average layer normal in the \hat{z} direction. $C(X,Y)$ is the surface height-height correlation function. This is related to the average roughness across the sample $g(X,Y) = \langle [z(X,Y) - z(0)]^2 \rangle$. For many isotropic solid surfaces $g(R) = (X^2 + Y^2)^{1/2} = AR^{2h}$ describing so-called self-affine roughness¹⁸. $h = D_H - 3$, where D_H is the fractal dimension of the surface. For systems of finite size (and measurement techniques with limited spatial resolution) $g(R) \rightarrow 2\sigma^2$ for large R , where σ is the rms roughness of the surface. A functional form satisfying these limits is

$$g(R) = 2\sigma^2 [1 - e^{-(R/\xi)^{2h}}].$$

ξ is a long-distance cutoff. Using this form for $g(R)$,

$$C(R) = \sigma^2 e^{-(R/\xi)^{2h}}.$$

$F(q_z)$ was determined by the specular portion of the rocking curves, the rms interlayer roughness σ , and the resolution function of the spectrometer. The fits are shown as solid lines in Fig. 2. *The agreement is excellent for all three rocking curves.* The data for all three quasi-Bragg peaks in Fig. 2 were fit using only *three significant adjustable parameters*: σ , ξ and h . Their values obtained from best fits are 3.6 ± 0.12 Å, 1327 ± 18 Å and 0.25 ± 0.05 , respectively. It should be mentioned that the wide range of q_z and q_x for the rocking curve data makes the fits extremely sensitive to the value of h . Figure 3, which plots the central portion of the 002 rocking curve with fits for three different values of h , demonstrates this sensitivity.

Thermally induced layer undulations also contribute to the diffuse scattering from the multilayer. To estimate this contribution, the layer displacement correlation function was calculated following Holyst⁶. Using the above values of B and K used to estimate L , and air/film and film/substrate interfacial tensions of 30 dyn/cm and 10 dyn/cm, respectively, the layer displacement correlation function, $\langle u_{ih}(R)u_{ih}(0) \rangle$ for the center of a 30-layer film is plotted in Fig. 5. Such thermal induced fluctuations are not conformal i.e. $C_{ij}(R)$ decays quickly for $i \neq j$ ⁶. Hence this estimate represents an upper limit. For comparison, the layer undulation correlation function determined by the fits to the data in Fig. 2 is also plotted.

Consider, instead the penetration of static undulations through the film. As stated above, the large value of the compression modulus in these liquid-crystal polymer films induces a large smectic penetration depth L . It is energetically less costly to propagate layer undulations parallel to the layer normal at the expense of in-plane director splay. Hence substrate roughness plays a major role in the smectic layer structure. The specular reflectivity of x-rays from the silicon substrate was measured to characterize its surface roughness. The substrate consists of a monolayer of octadecyltrichlorosilane (OTS) chemisorbed to the native oxide of a polished (100) silicon wafer. This data is shown in Fig. 4, along with the corresponding electron density profile. The data and fit agree very well with previous results on OTS coated silicon obtained by Tidswell et al.³ The modeling technique has been thoroughly discussed in Ref. [3]. The analysis yields an alkyl chain region with a density $\rho/\rho_{Si} = 0.38 \pm 0.03$ and a thickness of 21 ± 0.5 Å, indicative of a well-formed monolayer with a maximum chain tilt of 22° . As is the case with homeotropic alignment of bulk liquid-crystal samples by alkylsilanes,

Figure captions:

Figure 1. Specular and off-specular scans for a 29-layer liquid-crystal polymer film. The latter has been offset by a factor of five for clarity. Four Bragg reflections (layer spacing $c=45.7 \text{ \AA}$) are evident in the specular data revealing a well ordered layer structure. The mosaic of the layer normal is limited to 0.07° . The q_z dependence of the amplitude of the subsidiary maxima is discussed in Ref. [1]. The off-specular scan was taken at a trajectory $q_x=0.006q_z$. Diffuse scattering, sharply peaked at q_z of the Bragg reflections, is evident. The width of these peaks are similar to the primary maxima of the specular scan, implying that the associated layer undulations are replicated layer to layer. Inset shows chemical structure of the copolymer.

Figure 2. Rocking scans across the (a) 001, (b) 002 and (c) 003 Bragg reflections of Fig. 1. The incident beam in (a) was attenuated to avoid detector saturation near the peak. Open circles denote experimental data. Solid lines represent best fits to the model described in the text.

Figure 3. Enlargement of data and best fits to the 002 rocking curve for different values of h . Solid line: $h=0.25$, short dashed line: $h=1$, dashed-dot-dot line: $h=2$. All fits have been convolved with instrumental resolution. Inset: interfacial undulation correlation functions determined from fits to the rocking curve data (circles) and calculated from the model of Holyst for thermal undulations (triangles). The latter, calculated at the midpoint of a 29-layer film with $K=1 \times 10^{-6} \text{ dyn}$, $B=2.5 \times 10^9 \text{ dyn/cm}^2$, $\gamma_{air/film}=30 \text{ dyn/cm}$ and $\gamma_{film/substrate}=10 \text{ dyn/cm}$. The compressibility of the interdigitated layer consisting of the side-chain mesogens and alkyl chains of the silanes, $B_0=2.5 \times 10^7 \text{ dyn/cm}^2$.

Figure 4. Specular reflectivity normalized to Fresnel reflectivity (open circles) and fit to the model of Ref. [3] (solid line). The corresponding electron density profile is shown in the inset.

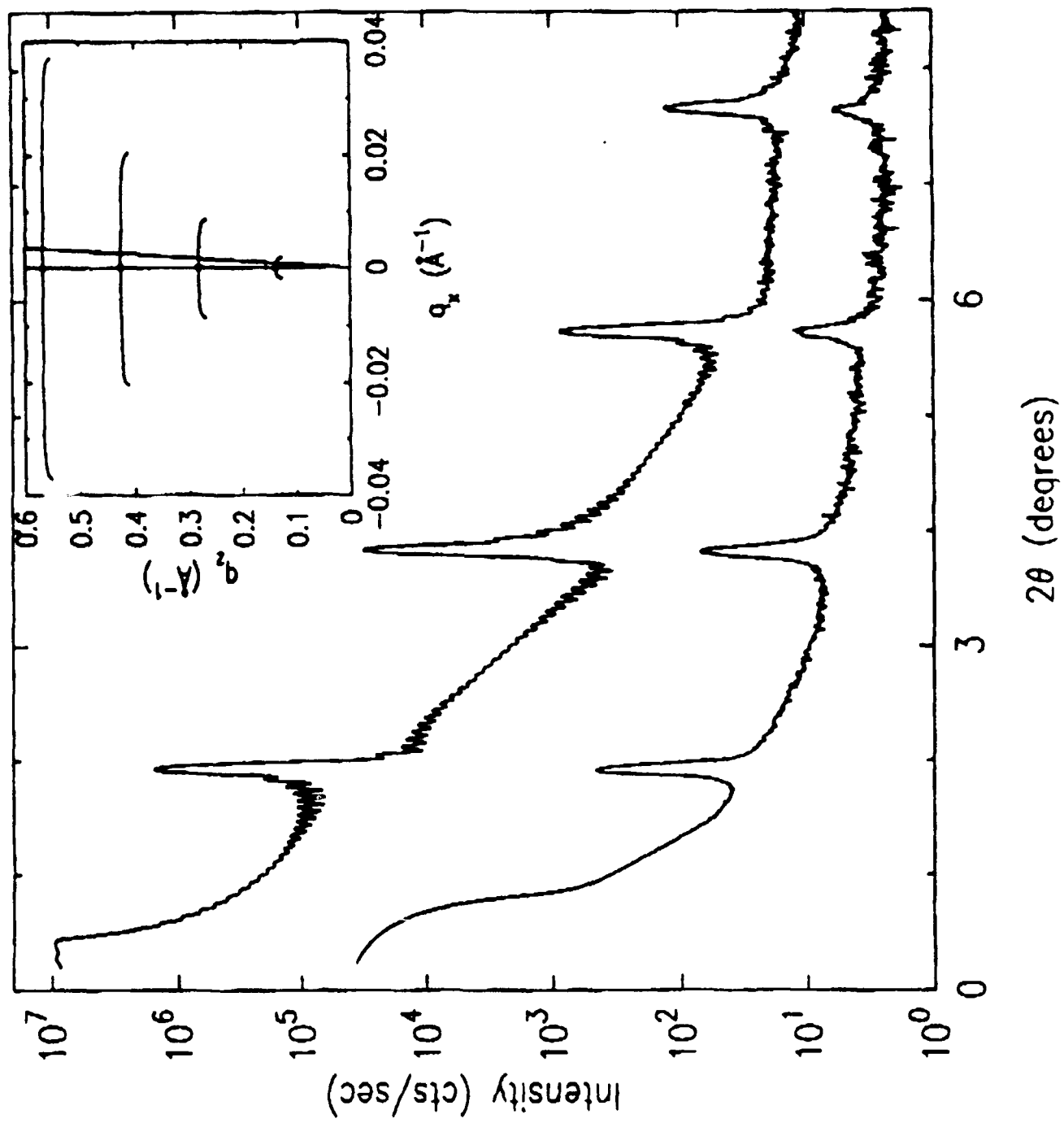
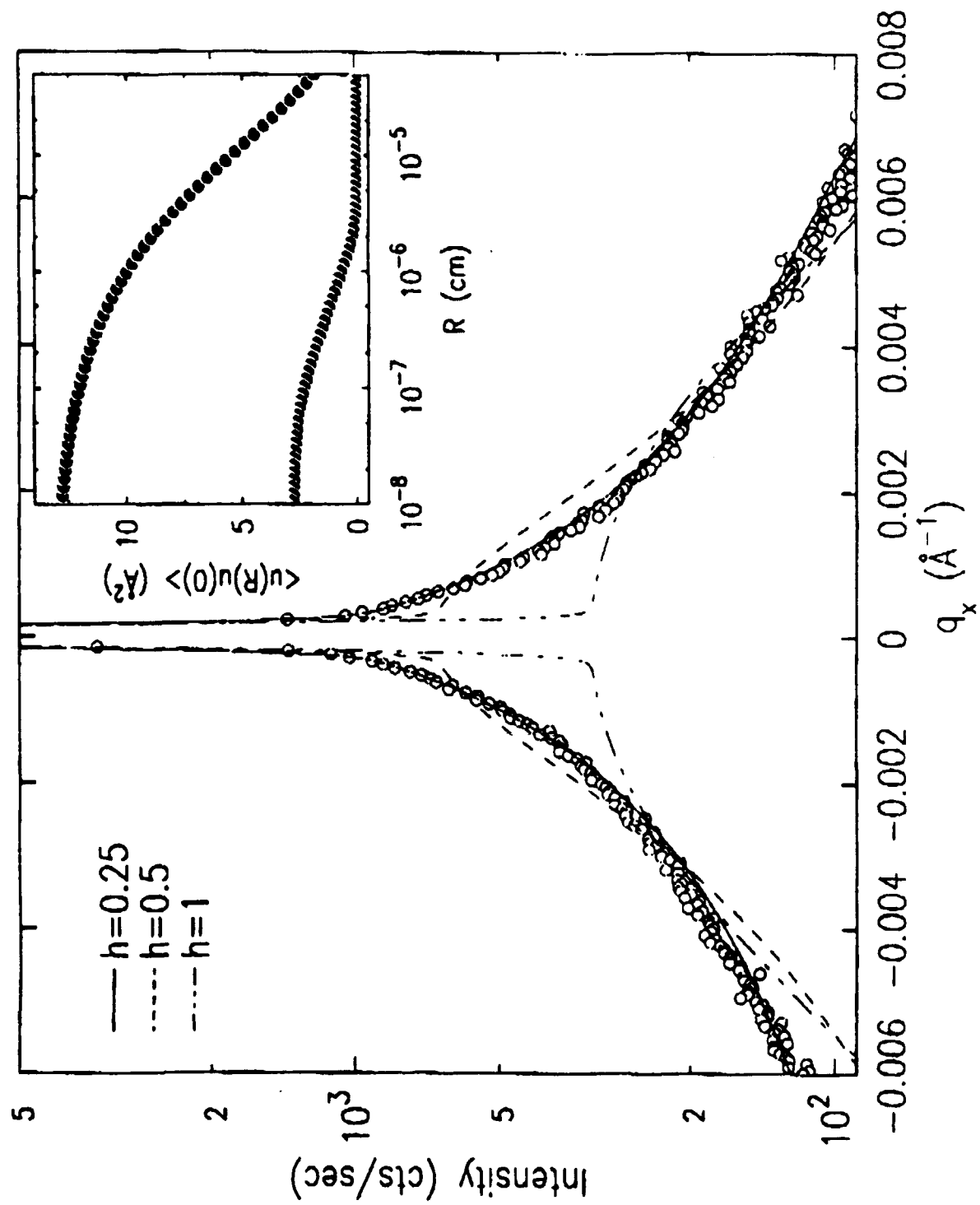


Fig. 1



Surface-Induced Static Undulations in Multilayer Films of Liquid-Crystalline Polymers

R. E. Geer and R. Shashidhar

Center for Bio/Molecular Science and Technology, Code 6900,
Naval Research Laboratory, Washington, D.C. 20375

A. F. Thibodeaux and R. S. Duran

Department of Chemistry, University of Florida, Gainesville, FL

Abstract

The first detailed study of surface-induced undulations in a liquid-crystalline polymer is presented. By examining the non-specular diffuse scattering from a 30-layer film of ferroelectric liquid-crystal polymer it is shown that the layer fluctuations are induced by the roughness of the film/substrate interface. This is in contrast to the case of free-standing films wherein thermal fluctuations play the major role.

Thin, smectic liquid-crystal films are of considerable current interest since they serve as model systems to study two-dimensional to three-dimensional crossover of inter- and intralayer order. For the most part, these studies have been on free-standing films. It is equally important to understand the influence of the interface between liquid-crystal films and the substrate. Film/vacuum and film/substrate interfaces are known to induce structural changes which are localized in the interfacial regions. On the other hand, such interfaces can also induce distinct thermodynamic phases as well as static undulations which penetrate into the interior of the film. The static undulations induced by roughness of the substrate surface has been studied in thin adsorbed films of cyclohexane. It was shown that for very thin films the substrate van der Waals interactions constrain the liquid surface to follow the static undulations of the substrate surface, while for thicker films the liquid surface structure is influenced mainly by thermally induced capillary waves. Early studies in homeotropically aligned smectic-

imperfections associated with the smectic layer order. Rocking scans through this diffuse scattering are shown in Fig. 2 for the first three Bragg peaks of Fig. 1. *These scans consist of broad diffuse scattering accompanied by a resolution limited peak due to specular reflection.* It may be recalled that Davidson and Levelut have reported similar diffuse bands perpendicular to the OOL axis for bulk samples of polysiloxane liquid-crystal polymers. These bands were attributed to undulations of longitudinally correlated rows of mesogens. The widths and amplitudes of the diffuse peaks of our LB multilayer shown in Fig. 1 are not consistent with such longitudinal undulations. We shall show that the diffuse scattering for the liquid-crystalline polymer is in fact due to static undulations of the smectic layers induced by the roughness of the substrate surface.

Quantitative analysis of the diffuse scattering of Fig. 2 is similar to that used by Sinha et al. for solid surfaces.⁷ For a single rough surface, the scattered intensity is given by

$$S(\vec{q}) = \frac{1}{q_z^2} \iint_{S_0} dX dY e^{q_z^2 C(X,Y)} e^{-i(q_x X + q_y Y)}.$$

X and Y are the Cartesian separations of two points on the surface S_0 with an average layer normal in the \hat{z} direction. $C(X,Y)$ is the surface height-height correlation function. This is related to the average roughness across the sample $g(X,Y) = \langle [z(X,Y) - z(0)]^2 \rangle$. For many isotropic solid surfaces $g(R = (X^2 + Y^2)^{1/2}) = AR^{2h}$ describing so-called self-affine roughness¹⁸. $h = D_H - 3$, where D_H is the fractal dimension of the surface. For systems of finite size (and measurement techniques with limited spatial resolution) $g(R) \rightarrow 2\sigma^2$ for large R , where σ is the rms roughness of the surface. A functional form satisfying these limits is

$$g(R) = 2\sigma^2 [1 - e^{-(R/\xi)^{2h}}].$$

ξ is a long-distance cutoff. Using this form for $g(R)$,

$$C(R) = \sigma^2 e^{-(R/\xi)^{2h}}.$$

$F(q_z)$ was determined by the specular portion of the rocking curves, the rms interlayer roughness σ , and the resolution function of the spectrometer. The fits are shown as solid lines in Fig. 2. *The agreement is excellent for all three rocking curves.* The data for all three quasi-Bragg peaks in Fig. 2 were fit using only *three significant adjustable parameters*: σ , ξ and h . Their values obtained from best fits are 3.6 ± 0.12 Å, 1327 ± 18 Å and 0.25 ± 0.05 , respectively. It should be mentioned that the wide range of q_z and q_x for the rocking curve data makes the fits extremely sensitive to the value of h . Figure 3, which plots the central portion of the 002 rocking curve with fits for three different values of h , demonstrates this sensitivity.

Thermally induced layer undulations also contribute to the diffuse scattering from the multilayer. To estimate this contribution, the layer displacement correlation function was calculated following Holyst⁶. Using the above values of B and K used to estimate L , and air/film and film/substrate interfacial tensions of 30 dyn/cm and 10 dyn/cm, respectively, the layer displacement correlation function, $\langle u_{ih}(R)u_{ih}(0) \rangle$ for the center of a 30-layer film is plotted in Fig. 5. Such thermal induced fluctuations are not conformal i.e. $C_{ij}(R)$ decays quickly for $i \neq j$ ⁶. Hence this estimate represents an upper limit. For comparison, the layer undulation correlation function determined by the fits to the data in Fig. 2 is also plotted.

Consider, instead the penetration of static undulations through the film. As stated above, the large value of the compression modulus in these liquid-crystal polymer films induces a large smectic penetration depth L . It is energetically less costly to propagate layer undulations parallel to the layer normal at the expense of in-plane director splay. Hence substrate roughness plays a major role in the smectic layer structure. The specular reflectivity of x-rays from the silicon substrate was measured to characterize its surface roughness. The substrate consists of a monolayer of octadecyltrichlorosilane (OTS) chemisorbed to the native oxide of a polished (100) silicon wafer. This data is shown in Fig. 4, along with the corresponding electron density profile. The data and fit agree very well with previous results on OTS coated silicon obtained by Tidswell et al.³ The modeling technique has been thoroughly discussed in Ref. [3]. The analysis yields an alkyl chain region with a density $\rho/\rho_{Si} = 0.38 \pm 0.03$ and a thickness of 21 ± 0.5 Å, indicative of a well-formed monolayer with a maximum chain tilt of 22° . As is the case with homeotropic alignment of bulk liquid-crystal samples by alkylsilanes,

Figure captions:

Figure 1. Specular and off-specular scans for a 29-layer liquid-crystal polymer film. The latter has been offset by a factor of five for clarity. Four Bragg reflections (layer spacing $c=45.7 \text{ \AA}$) are evident in the specular data revealing a well ordered layer structure. The mosaic of the layer normal is limited to 0.07° . The q_z dependence of the amplitude of the subsidiary maxima is discussed in Ref. [1]. The off-specular scan was taken at a trajectory $q_x=0.006q_z$. Diffuse scattering, sharply peaked at q_z of the Bragg reflections, is evident. The width of these peaks are similar to the primary maxima of the specular scan, implying that the associated layer undulations are replicated layer to layer. Inset shows chemical structure of the copolymer.

Figure 2. Rocking scans across the (a) 001, (b) 002 and (c) 003 Bragg reflections of Fig. 1. The incident beam in (a) was attenuated to avoid detector saturation near the peak. Open circles denote experimental data. Solid lines represent best fits to the model described in the text.

Figure 3. Enlargement of data and best fits to the 002 rocking curve for different values of h . Solid line: $h=0.25$, short dashed line: $h=1$, dashed-dot-dot line: $h=2$. All fits have been convolved with instrumental resolution. Inset: interfacial undulation correlation functions determined from fits to the rocking curve data (circles) and calculated from the model of Holyst for thermal undulations (triangles). The latter, calculated at the midpoint of a 29-layer film with $K=1 \times 10^{-6} \text{ dyn}$, $B=2.5 \times 10^9 \text{ dyn/cm}^2$, $\gamma_{\text{air/film}}=30 \text{ dyn/cm}$ and $\gamma_{\text{film/substrate}}=10 \text{ dyn/cm}$. The compressibility of the interdigitated layer consisting of the side-chain mesogens and alkyl chains of the silanes, $B_o=2.5 \times 10^7 \text{ dyn/cm}^2$.

Figure 4. Specular reflectivity normalized to Fresnel reflectivity (open circles) and fit to the model of Ref. [3] (solid line). The corresponding electron density profile is shown in the inset.

TECHNICAL REPORT DISTRIBUTION LIST - GENERAL

Office of Naval Research (2)
Chemistry Division, Code 1113
800 North Quincy Street
Arlington, Virginia 22217-5000

Dr. Richard W. Drisko (1)
Naval Civil Engineering
Laboratory
Code L52
Port Hueneme, CA 93043

Dr. James S. Murday (1)
Chemistry Division, Code 6100
Naval Research Laboratory
Washington, D.C. 20375-5000

Dr. Harold H. Singerman (1)
David Taylor Research Center
Code 283
Annapolis, MD 21402-5067

Dr. Robert Green, Director (1)
Chemistry Division, Code 385
Naval Weapons Center
China Lake, CA 93555-6001

Chief of Naval Research (1)
Special Assistant for Marine
Corps Matters
Code 00MC
800 North Quincy Street
Arlington, VA 22217-5000

Dr. Eugene C. Fischer (1)
Code 2840
David Taylor Research Center
Annapolis, MD 21402-5067

Defense Technical Information
Center (2)
Building 5, Cameron Station
Alexandria, VA 22314

Dr. Elek Lindner (1)
Naval Ocean Systems Center
Code 52
San Diego, CA 92152-5000

Commanding Officer (1)
Naval Weapons Support Center
Dr. Bernard E. Douda
Crane, Indiana 47522-5050

* Number of copies to forward